



# Effect of Knudsen Number, Lid Velocity and Velocity Ratio on Flow Features of Single and Double Lid Driven Cavities

S. Mukherjee<sup>1</sup>, V. Shahabi<sup>2</sup>, R. Gowtham Raj<sup>1</sup>, K. S. Rajan<sup>1</sup> and R. K. Velamati<sup>1†</sup>

<sup>1</sup>*Department of Mechanical Engineering, Amrita School of Engineering, Coimbatore, Amrita Vishwa Vidyapeetham, India*

<sup>2</sup>*High Performance Computing (HPC) Laboratory, Department of Mechanical Engineering, Ferdowsi University of Mashhad, 91775-1111, Mashhad, Iran*

†*Corresponding Author Email: v\_ratnakishore@cb.amrita.edu*

(Received July 3, 2018; accepted December 25, 2018)

## ABSTRACT

Effects of Knudsen number, lid velocity and velocity ratio are investigated on the flow features of single lid driven cavity with an aspect ratio of one and double lid driven cavity of aspect ratio two. Knudsen numbers studied are 0.01 (early slip regime), 0.1 (slip regime) and 1 (transitional regime). Lid velocities investigated are 100 m/s, 200 m/s and 500 m/s. The velocity ratios explored are 1 and -1. Knudsen number was found to have a huge impact on the flow rigidity. Lid velocity tends to shift the central vortex to the top left of the cavity for a cavity with aspect ratio of one and shifts the upper vortex to the top left of the cavity for a cavity with aspect ratio of two. Lid velocity does not affect the slip to a great extent on the lid. Changing the velocity ratio from 1 to -1 leads to the reversal of the relative vorticity in the top and bottom half of the cavity.

**Keywords:** Rarefied gas dynamics; DSMC; OpenFOAM; MEMS/NEMS.

## NOMENCLATURE

$Kn$	Knudsen number	$\zeta$	shear stress
$L$	characteristic length of the cavity	$\lambda$	mean free path
$U_{wall}$	lid velocity		
$T$	temperature		

## 1. INTRODUCTION

Micro/Nano electro mechanical systems (MEMS/NEMS) are extensively utilized in many application areas including semi-conductor coatings and biomedical devices. Hence, the study of gaseous flows in micro and nano scales has been an interesting and appealing topic of research in recent years. It is known that the Navier-stokes equation loses its validity at the micro/nano scales (Cercignani, 2000). Knudsen number, defined as the ratio of the mean free path ( $\lambda$ ) to the characteristic length ( $L$ ) in a flow is a very important dimensionless parameter used for defining the regime of the flow. For  $Kn < 0.001$ , it is the continuum regime, for  $0.001 < Kn < 0.1$  is the slip regime, for  $0.1 < Kn < 10$  is the transition regime and for  $Kn > 10$ , it is free molecular regime

(Bird, 2013). To effectively solve these type of flows, many formulations have been suggested over the past. In order to account for the slip in the velocity and temperature that are observed in the early slip regime, different slip models have been suggested (Zhang, Meng *et al.*, 2012). These slip models can be coupled with the Navier Stokes equation to obtain a valid solution. But, at even higher degrees of rarefaction, it becomes difficult to account for the large slips using mathematical models and a viable solution can be obtained only by resorting to the particle approach and solving the Boltzmann equation. The most widely used discretization of the Boltzmann equation is the lattice Boltzmann method, where the equations are solved at each lattice point (Mohamad, 2011). It is an arduous task to solve the entire Boltzmann equation and

as a result, different approximations of the Boltzmann equation have been suggested in the past. One such approximation is the Bhatnagar-Gross-Krook model (Patil, Lakshmisha *et al.*, 2006). This approach suggests that we assume the distribution of the particles at any given time to be slightly perturbed from the equilibrium distribution. Another popularly used approximation is the discrete velocity approach (Naris and Valougeorgis, 2005). Here, the velocity distribution is assumed to be discrete and is summed up over the given domain instead of a continuous integral. The most widely used and computationally feasible approach that is used to solve the Boltzmann equation the Direct Simulation Monte Carlo (DSMC) method (Bird, 2013). In this approach, a bunch of particles is taken as a lump and the Boltzmann equation is solved for them. This is a very effective method and has been known to give satisfactory result for a wide range of situation (Liou and Fang, 2001, John, Gu *et al.*, 2010, Darbandi and Roohi, 2011, Mohammadzadeh, Roohi *et al.*, 2011, Mohammadzadeh, Roohi *et al.*, 2012, Mohammadzadeh, Roohi *et al.*, 2013, White, Borg *et al.*, 2013).

The lid driven cavity is one of the most widely studied problem in the field of computational fluid dynamics as it shows a huge variety of flow properties and for this reason is used as a benchmarking problem for new CFD formulations. A thorough review has been done on the lid driven cavity at the macro scale (Shankar and Deshpande, 2000). They have shown the effects of various parameters like lid velocity, aspect ratio, geometry, Reynold's number etc., on the flow behaviour. The lid driven cavity at the micro/nano scale has been studied for small Reynold's number and small Mach numbers (Falmagne and Doignon, 2010). It has been reported that the vortex center moves vertically upward with increasing Knudsen number and stabilises after a certain critical value of Knudsen number. This phenomenon is justified by saying that as rarefaction increases the mass flux reduces and thus the vortex stabilizes. Lid driven cavities have been studied over a wide range of Knudsen numbers and the slip phenomenon is observed by (Naris and Valougeorgis (2005). Effects of rarefaction on cavity flow in the slip regime has also been studied by Mizzi *et al.*, (2007) They showed the failure of Navier Stokes equation to predict the flow behaviour at this regime. A detailed investigation of thermal and hydrodynamic flow behaviour of micro/nano cavities has been done by Roohi *et al.* (2011). They show different flow phenomena like cold to hot heat transfer, temperature and velocity jumps and also the variation of the DSMC solution from the Navier Stokes solution at large Knudsen numbers. The cold to hot heat transfer phenomenon has been justified by Roohi *et al.* (2011) using the concept of entropy flux (Roohi *et al.* (2011) .

Studies have been done on double lid driven

cavities at macro scale (Zhou, Patnaik *et al.*, 2003) using the continuum approach to solve the problem using the Navier Stokes equations with the variation of the speed and aspect ratios. This study has also been extended (Gürçan, 2003) to explore flow bifurcation in deep cavities. Sturges (Gürçan, 2003) is one of the earliest contributors to this domain and has shown experimental results to plot stream functions and pressure contours. Gaskell *et al.* (1998) extend their previous study to free surface side walls. However, this is an approximation of the Stokes flow between the coating caused by moving rolls. They use the continuum approach to find the stagnation points and eddies at aspect ratios less than 1. They find that the flow bifurcates, forming symmetric eddies when the speed ratio is unity. However, their findings also show that the flow can produce side eddies or smaller eddies. They have plotted bifurcation curves on a regime diagram which outlines all their findings.

Based on the literature survey, it can be seen that significant work has been on lid driven cavity at micro/nano scale. Also, at macro scale level studies are conducted on variation lid driven cavity like multiple lids driven cavity, cavities of various shapes etc. The current study focuses on exploring the double lid driven cavities of aspect ratio two in the micro/nano scales and comparing them to their single lid driven cavity of aspect ratio one counter part. The Knudsen number was varied from 0.01 to 1. The main focus is to understand how similar flow features between single and double lid driven cavity are.

## 2. THE DSMC METHOD

Bird's DSMC algorithm (Bird, 2013, Roohi and Stefanov, 2016) is a particle based approach based on the kinetic theory of gases. In this method, a number of real molecules are clustered together in order to represent a simulated particle, usually referred to as a DSMC particle. An important point here is that the time step should be less than the mean collision time at the given conditions. This is so that the decomposition of the movement and collision of the DSMC particles take place in an effective manner. The basic idea behind the algorithm is that the domain is first divided into cells which serve as boundaries for sampling and calculation of macroscopic properties. This cell is further divided into subcells which are used for the selection of collision partners. The molecular model used here is the Variable Hard Sphere (VHS) as it accounts for the change in viscosity with the temperature. A detailed review of this model is given by Matsumoto, (2003). The selection of collision pairs is done based on the No Time Counter (NTC) method where the time required for computation is directly proportional to the total number of DSMC particles in the domain. A generalized scheme of the no-time-counter scheme for the DSMC in rarefied gas flow analysis is given by Abe (1993). The major steps in the DSMC method consist of initialising,

moving the particles, indexing the DSMC particles, making collisions and then finally sampling the DSMC particles to calculate the macroscopic properties. In this study, an improved DSMC solver of the OpenFOAM software package (Scanlon, Roohi *et al.*, 2010), dsmcFoam+ (White, Borg *et al.* 2018) has been used. An i7 workstation with parallel dsmcFoam+ code has been used to compute flow in nano/micro lid driven cavity and each computation has taken 3-4 days on computation.

In the present work, monoatomic argon with a mass of  $6.63 \times 10^{-26}$  kg and a diameter of  $4.17 \times 10^{-10}$  m has been used. Fundamentally, any macroscopic property (F) is averaged over neighbouring cells as shown in equation 1. The time step used in this work is roughly about one third the mean collision and the number of DSMC particles per cell is about 30 as suggested by Bird (2013).

$$\bar{F}(N) = \frac{F(N) + \sum_{I=1}^{I=N_{Neighbour}} F_I}{N_{Neighbour} + 1} \quad (1)$$

### 3. RESULTS AND DISCUSSION

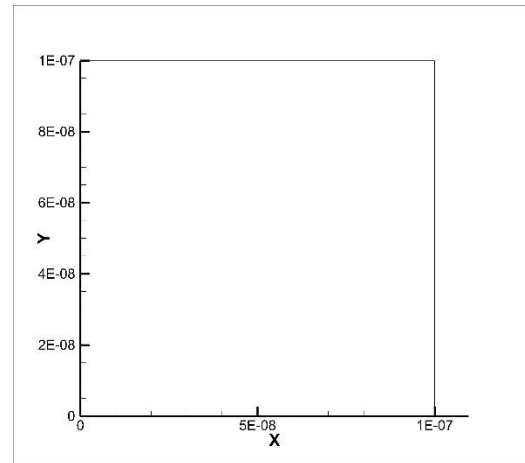
This study involves the study of two different cavity geometries as shown in Fig. 1. Figure 1(a) shows the single lid driven cavity of aspect ratio 1. Figure 1(b) shows the double lid driven cavity of aspect ratio 2. The double lid driven cavity is further classified according to the velocity ratio which is the ratio of the velocities of the top and bottom walls. A ratio of 1 indicates that both the lids move in the same direction while a ratio of -1 indicates that the lids move in opposite directions. The sides of the cavity in Fig. 1(a) are  $0.1 \times 0.1 \mu\text{m}$  whereas in Fig. 1(b) are  $0.2 \times 0.1 \mu\text{m}$ .

#### 3.1 Grid Independence and Code Validation

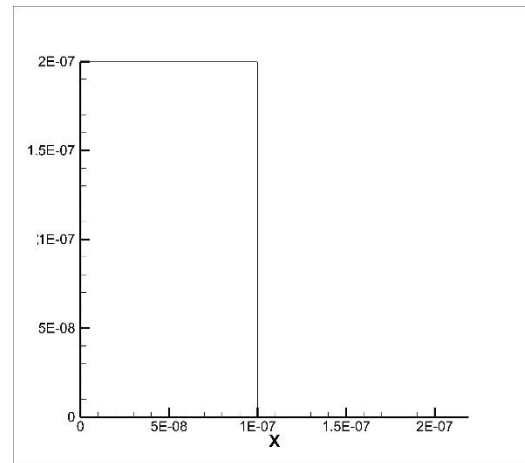
In order to use the code proposed for further simulations, it is necessary to first validate it. Validation is done with a case used in a work by Roohi *et al.* (2011). The micro cavity used for this case is same as Fig. 1(a). The Knudsen number used in this case is 0.5, which is in the early transition regime. All the walls are treated as diffuse and maintained at 300K. The top wall is moved with a velocity of 100 m/s. Figure 2 shows the comparison between the centerline velocities and temperatures obtained by Roohi *et al.* (2011) and the ones obtained in the course of this work. Temperature is validated along with velocity as it is a higher moment of the kinetic energy of the particles.

Three grids have been chosen for this validation case,  $50 \times 50$ ,  $100 \times 100$  and  $200 \times 200$ . The comparison of the centerline velocities for both the grids have been shown in Fig. 2. It is seen that the  $200 \times 200$  results match reasonable well with those obtained from a  $100 \times 100$  grid. Thus, for the rest of

this work, cells of similar size have been used in order to save computational time.



(a)



(b)

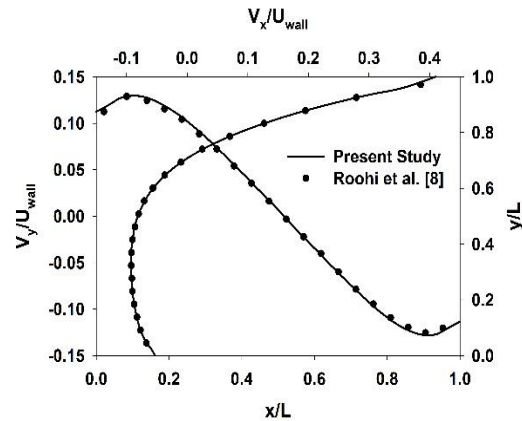
**Fig. 1. Cavity geometries investigated in this study.**

#### 3.2 Effect of Knudsen Number

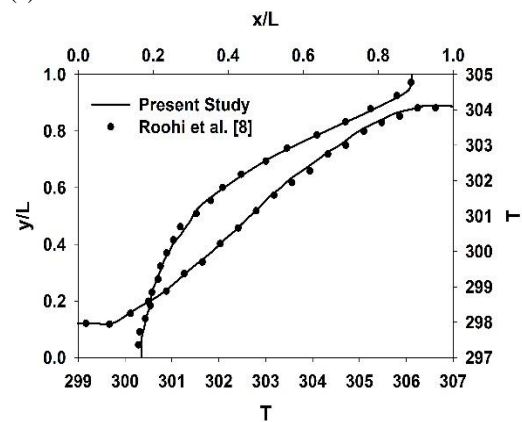
In order to investigate the effect of Knudsen number, the lid velocity for both the cavities are fixed at 100 m/s and the velocity ratio for the deep cavity is fixed at 1. The various Knudsen numbers investigated in this section are 0.01 (early slip regime), 0.1 (slip regime) and 1 (transition regime). In order to understand the flow features, several parameters are chosen to be examined as discussed further in this section.

Figures 4(a) and 4(b) show the velocity profiles along the horizontal and vertical center lines respectively. Figure 4(a) shows that the velocity profiles keep getting flatter as the Knudsen number increases. This can be attributed to the increased degree of rarefaction. The increased rarefaction results in less number of particles for transport to occur. This reduced transport is reflected in the flatter velocity profiles. Another important result that is derived from Fig. 4(a) is the comparison of double and single lid driven cavities. As the Knudsen number increases, the velocity profiles of the single and double lid driven cavities become

more and more similar. This can be attributed to the rigidity of the flow, which increases with the rarefaction.

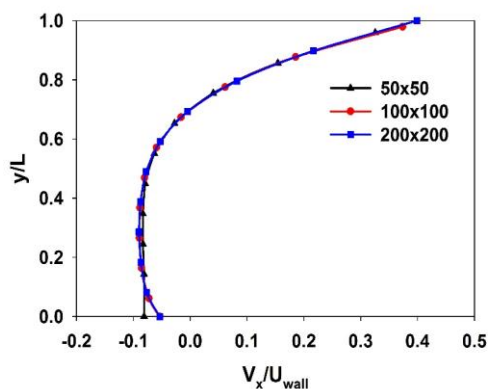


(a)



(b)

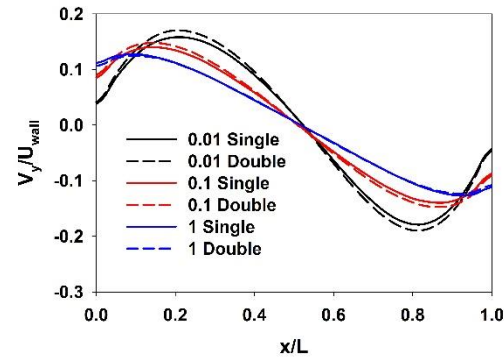
**Fig. 2. Validation against Roohi et al. (a) Velocity along the horizontal and vertical centerline (b) Temperature along the horizontal and vertical centreline.**



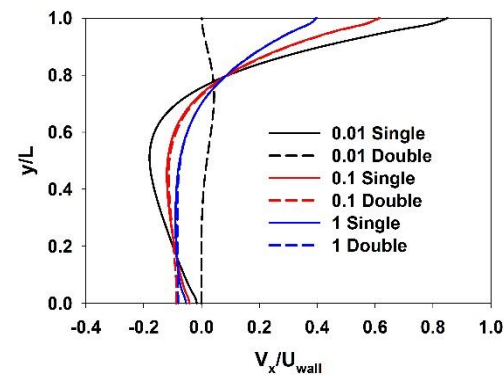
**Fig. 3. Grid independence.**

Figure 4(b) shows the velocity profiles along the vertical centerlines. As observed with the horizontal velocity profiles, a similar trend of flattening is observed here. This can again be attributed to the increased rarefaction. The comparison between the single and double lid driven cavities in this case is also shown in Fig. 4(b). In the case of early slip regime ( $Kn = 0.01$ ), absolutely no similarity is

observed between the single and double lid driven cavities. This is predominantly a result of the continuum characteristics of the flow which eventually fades out in the transition regime ( $Kn = 1$ ) evident from Fig. 4(b).



(a)



(b)

**Fig. 4. Velocity along the centerlines. (a) Velocity along the horizontal centerline. (b) Velocity along the vertical centreline.**

Figures 5(a) and 5(b) show the temperature profiles along the horizontal and vertical centerlines respectively. It is observed from Fig. 5(a) that the difference between the temperatures in the left and right corners increases with the Knudsen number. This can be attributed to the local compression on the right side and local expansion on the left side of the cavity as a result of the lid motion. The degree of this expansion and contraction increases as the rarefaction increases. This is due to the vanishing continuum characteristics of the flow with the increasing Knudsen number. Unlike the trends observed in Figs. 4(a) and 4(b), here the difference between the profiles tend to increase as the Knudsen number increases. This can be attributed to the increased rarefaction and thus increased the rigidity of the flow.

Figure 5(b) shows the temperature profiles along the vertical centerline. It is observed that there is a slight bend in the profiles for early slip regime ( $Kn = 0.01$ ) and slip regime ( $Kn = 0.1$ ), which is absent in the case of transition regime ( $Kn = 1$ ). This can be attributed to the temperature jump and slipping on the lid. In the first two cases, the effects due to this slip is eventually phased out

due to the momentum transfer through the rest of the fluid. But this is not observed in the last case as the medium is too rarefied for momentum transfer to occur. The comparison between single and double lid driven cavities is also observed in Fig. 5(b). Here it is observed that at the bottom most point along the vertical centerline (centerline in the case of double lid driven cavity), the difference in temperature is maximum for early slip regime ( $Kn = 0.01$ ) and minimum for transition regime ( $Kn = 1$ ). This can be attributed to the increasing rigidity of the flow due to less number of particles, with the increasing Knudsen number.

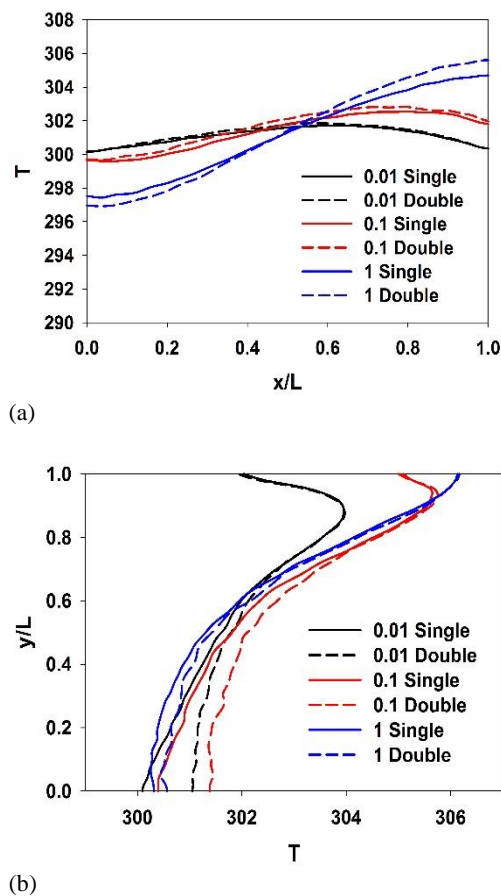


**Fig. 5. Temperature along the centerlines. (a) Temperature along the horizontal centerline. (b) Temperature along the vertical centreline.**

Figure 6 shows the non-dimensional shear stress along the horizontal centerline. It is non-dimensionalised by dividing with  $\rho \square$  thus it makes sense to compare among different Knudsen numbers. Thus, this graph shows the ratio of number of collisions to that of the number of molecules available. It is observed that there is an asymmetry in the shear profile for the transition regime ( $Kn = 1$ ). This can be attributed to the compression and expansion on the right and left side of the cavity respectively. Also, a comparison is drawn between the single and

double lid driven cavities. A trend similar to that observed in the temperature profile is observed, that is the similarity between the two decreases with increase in Knudsen number. In this comparison, it is observed that the ratio of the minimum non-dimensional shear stress along the horizontal centerline is 1.035 for  $Kn = 0.01$ , 1.068 for  $Kn = 0.1$  and 0.933 for  $Kn = 1$ . This can be attributed to the effectiveness of an imaginary “pseudo wall” formed in the case of the double lid driven cavity right at its geometric horizontal center. The effectiveness of this wall directly depends on the number of particles present. Thus, for a lower Knudsen, the pseudo wall formed is effective and for a higher Knudsen number, a weak pseudo wall is formed. This is the reason as to why shear is more in double lid driven cavity when compared to single lid driven cavity for lower Knudsen numbers.

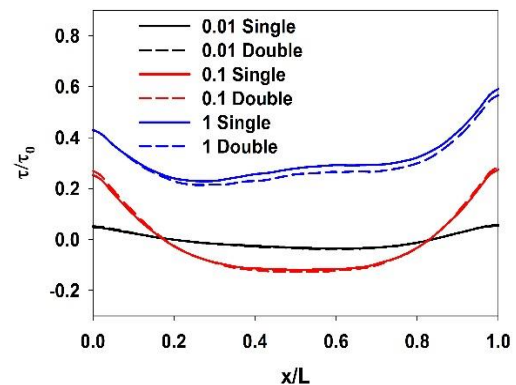


**Fig. 6. Shear stress along the horizontal centreline.**

### 3.3 Effect of lid velocity

In order to investigate the effect of lid velocity, the Knudsen number is fixed at 1 and the cavities as shown in Figs. 1(a) and 1(b) are used. The velocity ratio is fixed at 1. The lid velocities investigated here are 100 m/s, 200 m/s and 500 m/s.

Figures 7(a) and 7(b) show the non-dimensional velocity profiles along the horizontal and vertical centerlines for both single and double lid driven cavities for three different lid velocities: 100, 200 and 500 m/s. It is evident from Fig. 7(a) that the velocity profile along the horizontal centerline becomes flat with the increase in lid velocity. This can be attributed to the vortex movement in the cavity. Heat lines are represented over the temperature contours for both single lid and double lid cavities for two different lid velocities in Figs. 8 (a-d). Temperature contours look similar but heat lines vary along the mid section for double lid cavity when compared with single lid cavity. It can also be observed that heat flows from hot to cold similar in both single and double lid cavities as observed by [Roohi et al. \(2011\)](#).

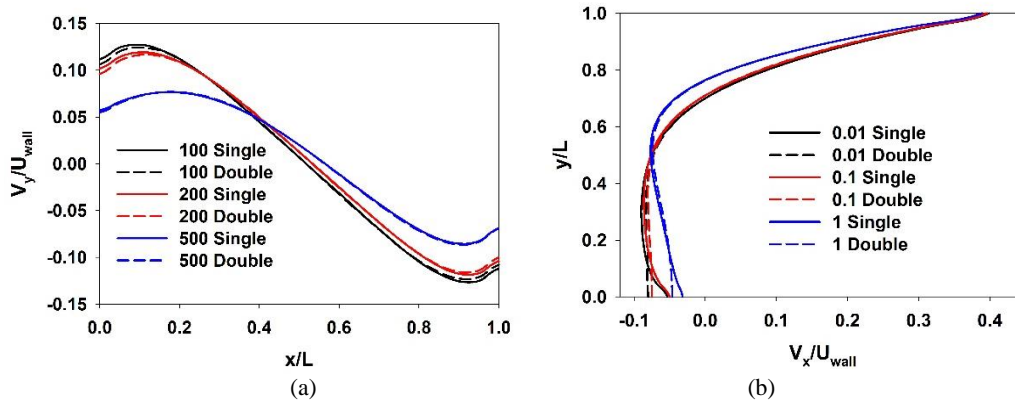


Fig. 7. Comparison of velocity profiles between different lid velocities for single and double lid driven cavities. (a) Along horizontal centerline (b) Along vertical centreline.

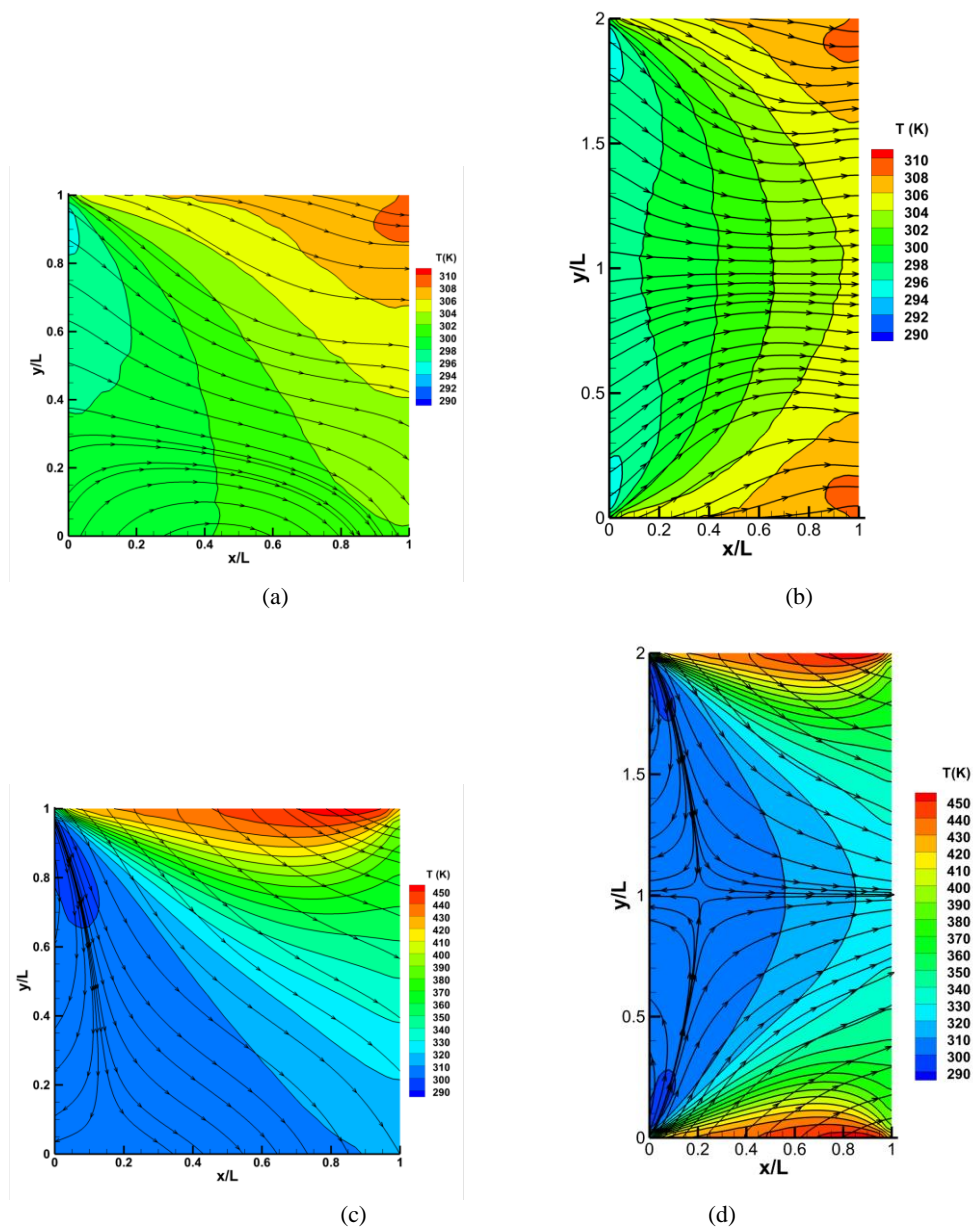
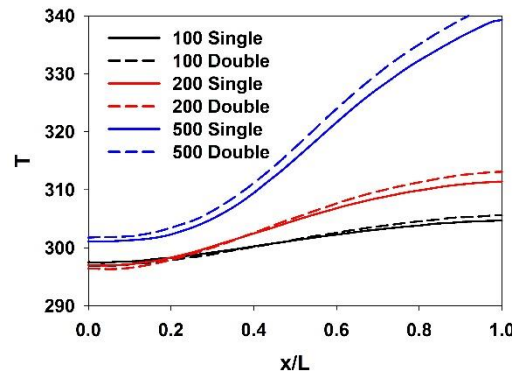
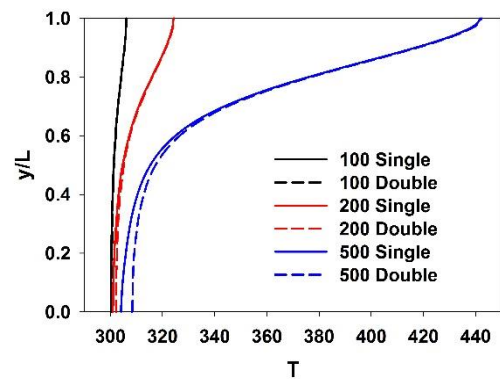


Fig. 8. Heat lines of heat flux on contours of temperature. (a) 100 m/s single lid driven cavity (b) 100 m/s double lid driven cavity (c) 500 m/s single lid driven cavity (d) 500 m/s double lid driven cavity.

It is observed that the vortex moves towards the top right corner as the lid velocity increases (in the case of single lid driven cavity and top half of the double lid driven cavity). This movement of the vortex to the top makes the velocity profile over the horizontal centerline flat. It because of the slip occurring at the lid is not dependent on the lid velocity but the Knudsen number.



(a)



(b)

**Fig. 9. Temperature profiles along the (a) horizontal centreline.**

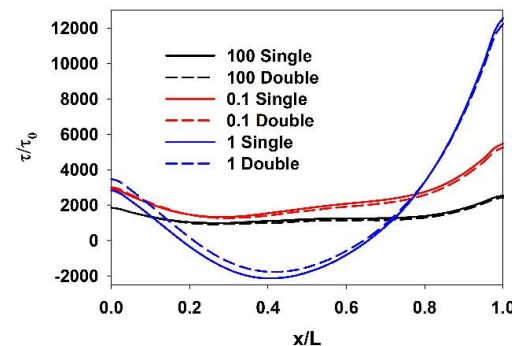


**Fig. 10. Shear stress profiles along the horizontal centreline.**

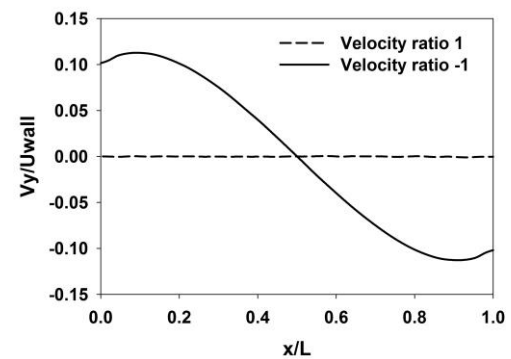
Figures 9(a) and 9(b) show the temperature profiles for both single and double lid driven cavities along the horizontal and vertical centerlines for three different lid velocities. It is evident from Fig. 9(a) that the temperature profiles become increasingly asymmetric as the lid velocity increases. This can be attributed to the increased expansion and compression effect on the top corners of the cavity.

This causes the temperature to rise up in the top right corner and go down in the bottom left corner. Figure 9(b) shows that the temperature on the right side of the lid increases enormously with an increase in the lid velocity. This is a result of the combined effects of increased viscous dissipation and compression effects.

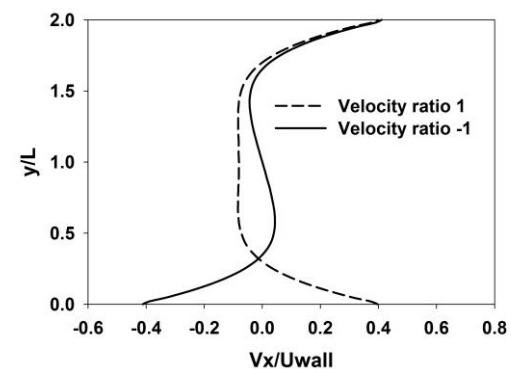
Figure 10 shows the shear stress profiles along the horizontal centerline. It is evident that the symmetry is increasingly disrupted with the increasing lid velocity. This is again a result of the increased viscous dissipation and compression/expansion. It is also observed that the shear stress in the central part of the cavity is decreasing with an increase in the lid velocity. This is a direct result of the increased inertia forces due to increasing lid velocity. An increase in the inertia force dominates the viscous forces and hence there is a drop in the shear stress.

### 3.4 Effect of Velocity Ratio

In order to investigate the effect of velocity ratio, the Knudsen number is fixed at 1. The lid velocity is fixed at 100 m/s and the aspect ratio is fixed at 2. The velocity ratios studied in this section are 1 and -1.



(a)

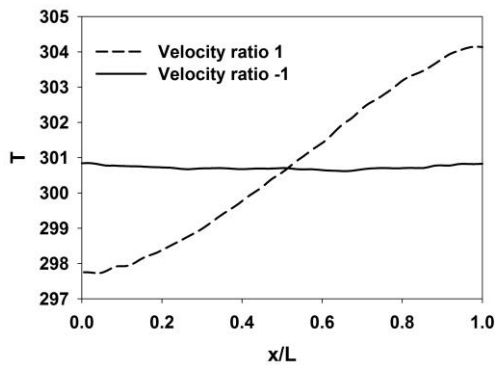


(b)

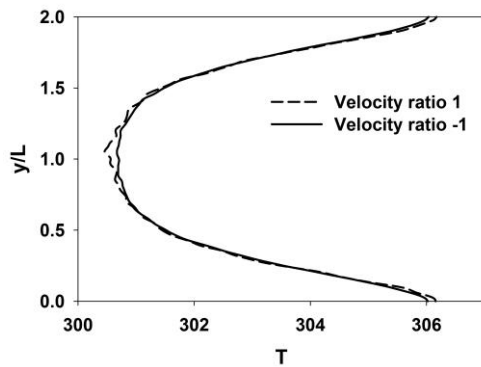
**Fig. 11. Velocity profiles of double lid driven cavities for different velocity ratios along (a) Horizontal centerline and (b) Vertical centreline.**

Figures 11(a) and 11(b) show the velocity profiles along the horizontal and vertical centerlines respectively. It is seen in Fig. 11(a) that the velocities along the horizontal centerline is zero all over for a

velocity ratio of 1. This can be explained using the velocity profile observed in Fig. 11(b) for a velocity ratio 1. It is seen that the velocity profile along the vertical centerline stays similar on the other half after the center for a velocity ratio of 1, whereas it flips for a velocity ratio of -1. This symmetry about the horizontal centerline for a velocity ratio of 1 is the reason for cancelling out the vertical velocities along the horizontal centerline. The velocity flip for a velocity ratio of -1 as shown in Fig. 11(b) causes a reversal in the vorticity directions in the top and bottom half of the cavity resulting in opposite vertical velocities along the horizontal centerline in the left and right half of the cavity.



(a)

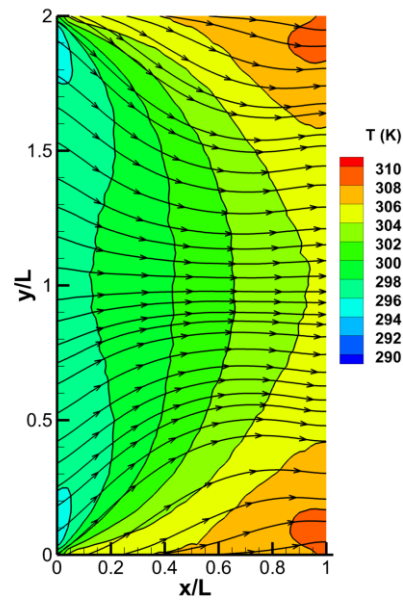


(b)

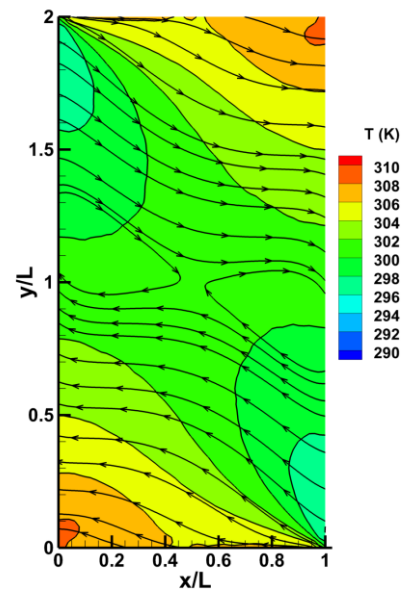
**Fig. 12. (a) Horizontal and (b) Vertical centerline temperatures for different velocity ratios,**

Figures 12(a) and 12(b) show the temperature profiles along the horizontal and vertical centerlines respectively, of the double lid driven cavities with velocity ratios of 1 and -1. It is observed from Fig. 12(b) that the temperature profiles along the vertical centerline for both the velocity ratios match well despite the difference in the lid velocities. This is so because temperature is a scalar unlike velocity. It is observed from Fig. 12(a) that the temperature along the horizontal centerline is flat and close to the equilibrium temperature of 300K for a velocity ratio of -1. This trend is explained using Fig. 13. Due to both the lid velocities being in the same direction (Fig. 13(a)), the compression occurs on the right side of the cavity both in the top and bottom. Similarly, the expansion occurs on the left side of the cavity. This makes the temperature along the horizontal centerline to be higher on the right side and lower

on the left side. But for a velocity ratio of -1 (Fig. 13(b)), the compression occurs on the right side and the expansion occurs on the left side in the top half and vice versa in the bottom half. Due to this mirrored nature, the temperature along the horizontal centerline remains more-or-less around the equilibrium temperature.



(a)



(b)

**Fig. 13. Heat lines of heat flux on temperature contours for velocity ratios of (a) 1 and (b) -1.**

#### 4. CONCLUSION

Effects of Knudsen number, lid velocity and velocity ratio on the flow features of single and double lid driven micro cavities of aspect ratios 1 and 2 respectively, have been investigated. Knudsen number is found to have a major effect on the flow rigidity based on the symmetry of single and

double lid driven cavities. An increase in lid velocity tends to move the central vortex to the top right of the cavity. Lid velocity does not seem to affect the flow symmetry between single and double lid driven cavities to a great extent. Changing the velocity ratio tends to flip the flow features about the horizontal centerline which further emphasizes that the flow is rigidified at that particular Knudsen number.

## REFERENCES

- Abe, T. (1993). Generalized scheme of the no-time-counter scheme for the DSMC in rarefied gas flow analysis. *Computers & Fluids* **22**(2), 253-257.
- Bilgil, H. and F. Gürcan (2016). Effect of the Reynolds number on flow bifurcations and eddy genesis in a lid-driven sectorial cavity. *Japan Journal of Industrial and Applied Mathematics* **33**(2), 343-360.
- Bird, G. A. (2013). *The DSMC Method*. CreateSpace Independent Publishing Platform.
- Cercignani, C. (2000). *Rarefied Gas Dynamics: From Basic Concepts to Actual Calculations*, Cambridge University Press.
- Darbandi, M. and E. Roohi (2011). DSMC simulation of subsonic flow through nanochannels and micro/nano backward-facing steps. *International Communications in Heat and Mass Transfer* **38**(10), 1443-1448.
- Falmagne, J. C. and J. P. Doignon (2010). *Learning Spaces: Interdisciplinary Applied Mathematics*, Springer Berlin Heidelberg.
- Gaskell, P. H., F. Gürcan, M. D. Savage and H. M. Thompson (1998). Stokes flow in a double-lid-driven cavity with free surface side walls. Proceedings of the Institution of Mechanical Engineers, Part C. *Journal of Mechanical Engineering Science* **212**(5), 387-403.
- Gürcan, F. (2003). Streamline Topologies in Stokes Flow Within Lid-Driven Cavities. *Theoretical and Computational Fluid Dynamics* **17**(1), 19-30.
- John, B., X. J. Gu and D. R. Emerson (2010). Investigation of Heat and Mass Transfer in a Lid-Driven Cavity Under Nonequilibrium Flow Conditions. *Numerical Heat Transfer, Part B: Fundamentals* **58**(5), 287-303.
- Liou, W. W. and Y. Fang (2001). Heat transfer in microchannel devices using DSMC. *Journal of Microelectromechanical Systems* **10**(2), 274-279.
- Matsumoto, H. (2003). Variable Sphere Molecular Model in the Monte Carlo Simulation of Rarefied Gas Flow. *Rarefied Gas Dynamics: 23rd International Symposium*. A. D. K. a. E. P. Muntz.
- Mizzi, S., D. R. Emerson, S. K. Stefanov, R. W. Barber and J. M. Reese (2007). Effects of rarefaction on cavity flow in the slip regime. *Journal of computational and theoretical nanoscience* **4**(4), 817-822.
- Mohamad, A. A. (2011). *Lattice Boltzmann Method: Fundamentals and Engineering Applications with Computer Codes*. Springer London.
- Mohammadzadeh, A., E. Roohi and H. Niazmand (2013). A Parallel DSMC Investigation of Monatomic/Diatomic Gas Flows in a Micro/Nano Cavity. *Numerical Heat Transfer, Part A: Applications* **63**(4), 305-325.
- Mohammadzadeh, A., E. Roohi, H. Niazmand, S. Stefanov and R. S. Myong (2012). Thermal and second-law analysis of a micro- or nanocavity using direct-simulation Monte Carlo. *Physical Review E* **85**(5), 056310.
- Mohammadzadeh, A., E. Roohi, H. Niazmand and S. K. Stefanov (2011). Detailed Investigation of Thermal and Hydrodynamic Flow Behaviour in Micro/Nano Cavity Using DSMC and NSF Equations. (44632): 341-350.
- Naris, S. and D. Valougeorgis (2005). The driven cavity flow over the whole range of the Knudsen number. *Physics of Fluids* **17**(9), 097106.
- Patil, D. V., K. N. Lakshmisha and B. Rogg (2006). Lattice Boltzmann simulation of lid-driven flow in deep cavities. *Computers & Fluids* **35**(10), 1116-1125.
- Roohi, E. and S. Stefanov (2016). Collision partner selection schemes in DSMC: From micro/nano flows to hypersonic flows. *Physics Reports* **656**, 1-38.
- Scanlon, T. J., E. Roohi, C. White, M. Darbandi and J. M. Reese (2010). An open source, parallel DSMC code for rarefied gas flows in arbitrary geometries. *Computers & Fluids* **39**(10), 2078-2089.
- Shankar, P. N. and M. D. Deshpande (2000). Fluid Mechanics in the Driven Cavity. *Annual Review of Fluid Mechanics* **32**(1), 93-136.
- White, C., M. K. Borg, T. J. Scanlon, S. M. Longshaw, B. John, D. R. Emerson and J. M. Reese (2018). dsmcFoam+: An OpenFOAM based direct simulation Monte Carlo solver. *Computer Physics Communications* **224**, 22-43.
- White, C., M. K. Borg, T. J. Scanlon and J. M. Reese (2013). A DSMC investigation of gas flows in micro-channels with bends. *Computers & Fluids* **71**, 261-271.
- Zhang, W.-M., G. Meng and X. Wei (2012). A review on slip models for gas microflows. *Microfluidics and Nanofluidics* **13**(6), 845-882.
- Zhou, Y. C., B. S. V. Patnaik, D. C. Wan and G. W. Wei (2003). DSC solution for flow in a staggered double lid driven cavity.